Received: 25 December 2018 | Revised: 10 December 2019 | Accepted: 3 January 2020

DOI: 10.1002/alz.12062

Alzheimer's & Dementia®
THE JOURNAL OF THE ALZHEIMER'S ASSOCIATION

FEATURED ARTICLE

Age-dependent amyloid deposition is associated with white matter alterations in cognitively normal adults during the adult life span

Miguel Á. Araque Caballero[1] | Zhuang Song[2] | Anna Rubinski[1] | Marco Duering[1] | Martin Dichgans[1,3] | Denise C. Park[2] | Michael Ewers[1]

[1]Institute for Stroke and Dementia Research, University Hospital, LMU Munich, Munich, Germany

[2]Center for Vital Longevity, University of Texas at Dallas, Dallas, Texas

[3]Munich Cluster for Systems Neurology (SyNergy), Munich, Germany

Correspondence
Dr. Michael Ewers, Institute for Stroke and Dementia Research, Klinikum der Universität München, Ludwig-Maximilians-Universität München, Feodor-Lynen-Straße D-81377 Munich, Germany.
Email: michael.ewers@med.uni-muenchen.de

Abstract

Introduction: Both beta-amyloid (Ab) deposition and decline in white matter integrity, are brain alterations observed in Alzheimer's disease (AD) and start to occur by the fourth and fifth decades. However, the association between both brain alterations in asymptomatic subjects is unclear.

Methods: Amyloid positron emission tomography (PET) and diffusion tensor imaging (DTI) were obtained in 282 cognitively normal subjects (age 30-89 years). We assessed the interaction of age by abnormal amyloid PET status (Florbetapir F-18 PET >1.2 standard uptake value ratio [SUVR]) on regional mean diffusivity (MD) and global white matter hyperintensity (WMH) volume, controlled for sex, education, and hypertension.

Results: Subjects with abnormal amyloid PET (n = 87) showed stronger age-related increase in global WMH and regional MD, particularly within the posterior parietal regions of the white matter.

Discussion: Sporadic Aβ deposition is associated with white matter alterations in AD predilection areas in an age-dependent manner in cognitively normal individuals.

KEYWORDS

Alzheimer's disease, amyloid β, diffusion tensor imaging, life span, mean diffusivity, white matter hyperintensities, white matter

1 | INTRODUCTION

White matter alterations are common in Alzheimer's disease (AD).[1] Although cortical neurodegeneration is a core feature of AD, several lines of research suggest that white matter impairment is part of the pathological cascade in AD.[2-5] Brain autopsy studies showed partial loss of axons, reduced myelin, and increased astrogliosis in the white matter in patients with pathological diagnosis of AD.[2,6] White matter hyperintensity volume, a gross radiological marker of white matter alterations, is increased in autosomal dominant AD, that is, genetically caused AD with an early onset of dementia symptoms.[7] These results suggest that pathological white matter changes are not merely due to aging but constitute a significant feature of AD. Studies using diffusion tensor imaging (DTI) showed that microstructural white matter alterations occur in a region-specific manner,[8,9] predominantly within posterior parietal white matter in very mild AD.[4,10-12] In autosomal dominant AD, we previously found that DTI-assessed mean diffusivity (MD) was increased predominantly in posterior parietal white matter

5-10 years before symptom onset.[13] Together these results suggest that white matter alterations occur in circumscribed brain regions at an early pre-symptomatic stage of AD.[14]

The deposition of cortical amyloid β (Aβ; henceforth we refer only to cortical Aβ) precedes the onset of Alzheimer's disease (AD) symptoms by >20 years,[15,16] typically beginning within the fourth or fifth decade of life.[17,18] Aβ deposition has been associated previously with small vessel disease in the form of capillary cortical amyloid angiopathy (CAA) and arteriosclerosis,[6,19,20] which may entail white matter damage.[6,21,22] These observations suggest that the Aβ deposition occurring during middle and older age is associated with accelerated age-related white matter alterations, even though the exact mechanisms remain unclear. Results from lifespan diffusion tensor imaging (DTI) studies suggest maturation of fiber tracts to continue until the fourth decade of life,[23] followed by decline in white matter integrity at a higher age.[23–25] Few studies, however, have assessed the association between early accrual of Aβ deposition and white matter decline in asymptomatic middle-aged and older adults.[4,26-29] In elderly cognitively normal subjects, higher Aβ deposition (as assessed by amyloid PET) was associated with DTI alterations within the splenium[30] and cingulum bundle.[31] In late middle-aged cognitively normal subjects, abnormal levels of Aβ have only inconsistently been associated with DTI alterations,[12,27,32,33] probably because the small sample size hampered statistical power.[12,32,33] Therefore, the question remains whether microstructural white matter alterations are associated with early cerebral amyloid deposition. In addition, there are few studies of middle-aged adults and it is not clear at what age these associations can be observed. We addressed these questions using a large sample of participants from the Dallas Lifespan Brain Study (DLBS), including 282 cognitively normal adults from age 30-89, allowing us to examine the association between deposition of Aβ and white matter alterations across the adult life span. Based on our previous findings of predominantly posterior parietal alterations of MD in autosomal dominant AD[13],[13] our primary hypothesis was that Aβ deposition is associated with a higher age-related increase of MD, particularly in posterior parietal and long-projecting frontoparietal fiber tracts.

RESEARCH IN CONTEXT

1. Systematic review: White matter alterations including white matter hyperintensities and microstructural white matter alterations are part of the pathological brain changes in Alzheimer's disease (AD), but may precede symptom onset by decades. Amyloid β (Aβ), a primary pathology of AD, starts to occur 20-25 years before symptom onset. Whether Aβ deposition is associated with white matter alterations in asymptomatic subjects already during middle and older age is unclear.
2. Interpretation: Our finding in cognitively normal subjects between 30 and 89 years suggested that increased amyloid positron emission tomography (PET) is already associated with the posterior parietal regions. These white matter changes were independent of hypertension and may thus stem from amyloid angiopathy in the brain.
3. Future directions: The current findings encourage future longitudinal investigations on the contribution of amyloid related white matter alterations to the development of dementia.

2 | METHODS

2.1 | Subjects

We studied 294 cognitively normal subjects from the or DLBS. Inclusion criteria required the individuals to be right-handed, native English speakers, a Mini Mental State Examination (MMSE) score of ≥26; available DTI, T1 MRI, and Florbetapir F-18 PET scans as well as completion of a cognitive test battery. The age range was between 30 and 89 years. Quality control prior and after pre-processing of T1 and DTI images resulted in the exclusion of 12 subjects due to anatomical abnormalities (abnormally enlarged ventricles: n = 1; abnormally enlarged subarachnoid spaces: n = 1) or artifacts/noise that prevented a successful pre-processing (DTI: n = 6, T1: n = 4), yielding a total of 282 subjects. Unless otherwise specified for a specific analysis, this was the final sample used for all statistical analyses. The two cognitive visits were a median of 3 days apart (interquartile range [IQR] = 5, min = 0, max = 69).

The MRI was acquired a median of 11 days after the second cognitive visit (IQR = 13, min = −7, max = 132). The PET was acquired a median of 82 days after the MRI (IQR = 202.2, min = −21, max = 593; only 19 subjects had their PET taken >1 year after the MRI).

Written informed consent was obtained according to the policy of the institutional review board of the University of Texas Southwestern Medical Center and the University of Texas at Dallas.

2.2 | Cognitive assessments

The overall cognitive status was assessed with MMSE. Composite scores of episodic memory and executive function were computed as described previously.[34] Briefly, for episodic memory, the number of correct items in the immediate and delayed tests of the Hopkins Verbal Learning Task and the number of items correctly remembered in the Verbal Recognition Memory task from the Cambridge Neuropsychological Test Automated Battery (CANTAB) were each *z*-score transformed. The average *z*-score across the tests was computed for each subject to yield the episodic memory composite score. For executive function, measures of processing speed (number of correct items on the Digit Symbol and Digit Comparison tasks) and working memory (number of correct items on the Letter-Number Sequencing task and sum of perfectly recalled trials on the Operation Span task) were each *z*-score transformed. The *z*-scores averaged across all of these tests yielded the executive function composite score.

2.3 | Assessment of hypertension

The hypertensive status of the patients in the DLBS has been reported previously.[18] Briefly, an individual was considered hypertensive if she/he had either a diagnosis of hypertension by her/his physician, or if the blood pressure, as obtained during the study, exceeded the criterion for stage 1 hypertension (systolic blood pressure >140 mm Hg or diastolic blood pressure >90 mm Hg). Blood pressure was measured twice at each of two cognitive visits, twice during the PET visit and once during the MRI visit. Measurements were obtained with an automatic sphygmomanometer (HEM-780; Omron) attached to the left arm of the participant who was either seated (cognitive visit) or in the supine position (PET visit). Systolic and diastolic blood pressure values were averaged across all seven visits.

2.4 | MRI acquisition

MRI scans were acquired by a Philips Achieva 3 T MR scanner (Philips Medical Systems, Best, The Netherlands). The T1-weighted images were acquired with an magnetization prepared rapid gradient echo (MPRAGE) sequence with 1 mm isotropic voxel size, repetition time (TR) = 8.18 ms, echo time (TE) = 3.76 ms, and flip-angle = 12°. Diffusion-weighted MRI was acquired using whole-brain T2*-weighted interleaved echo-planar imaging (EPI) with 2 mm isotropic voxel size, TR = 4410 ms, TE = 51 ms, flip-angle = 90°, and 1 mm slice gap. One b = 0 volume and 30 diffusion directions were recorded with b = 1000 s/mm^2. T2–fluid-attenuated inversion recovery (FLAIR) scans were acquired axially (repetition time = 11,000 ms, echo time = 125 ms, flip angle = 120°) with 0.45 mm × 0.45 mm × 5.96 mm voxel size.

2.5 | β Amyloid PET

Amyloid deposition was measured by scanning participants in a Siemens ECAT HR PET Scanner using Florbetapir F-18. The scan began 50 minutes after injection of a 370 MBq (10 mCi) dose of the Florbetapir F-18 radiotracer. A two-frame × 5-minute dynamic emission acquisition was performed, reconstructed using back-projection. The scans were spatially normalized to a Florbetapir F-18 template in Montreal Neurological Institute (MNI) (2 mm isotropic resolution), and a 6 mm full width at half maximum (FWHM) Gaussian filter was applied. The computation of global Florbetapir F-18 followed a procedure described previously for Florbetapir F-18 PET scans in the DLBS study.[35] The radiotracer uptake was averaged across voxels within each of eight predefined cortical regions of interest (ROIs), including the dorsolateral prefrontal cortex, orbitofrontal cortex, lateral parietal cortex, posterior and anterior cingulate, precuneus, lateral temporal cortex and occipital cortex.[34-36] For each subject and ROI, the average PET values were normalized to the whole cerebellum to compute standard uptake value ratios (SUVR); these PET values were averaged across the eight ROIs to obtain the global SUVR score.[35]

2.6 | Amyloid β status

Subjects were classified into two groups based on the global SUVR score, which provided a measure of the magnitude of Aβ uptake in the brain. Amyloid positivity (Aβ+) was thresholded at a global SUVR ≥1.2, as established previously,[35] and participants with a lower global SUVR score were termed amyloid negative (Aβ−).

2.7 | DTI pre-processing

The diffusion-weighted volumes and the b = 0 reference volume were pre-processed by a standard procedure implemented in the ExploreDTI toolbox (http://www.ExploreDTI.com).[37] In particular, the DTI scans were corrected for subject motion and eddy currents, and the same transformations that were applied to the diffusion-weighted volumes were also applied to the B-matrix of diffusion directions.[38] For each subject, the thus corrected DTI scan was adjusted subsequently for susceptibility distortions by nonlinear registration to the subject's brain-extracted T1 volume, using the Explore DTI toolbox.[39] A particular feature of this procedure is that the deformations can be restricted to the phase-encoding direction of the DTI scan (ie, the anterior-posterior direction in our case). Finally, diffusion-tensor estimation by ordinary least-squares was carried out to generate fractional anisotropy (FA as required for tract-based spatial statistics [TBSS], see next section) and MD maps for each subject.

2.8 | Tract-based spatial statistics

The MD maps were superimposed onto a white matter skeleton template, using TBSS[40] included in the FSL toolbox (https://fsl.fmrib.ox.ac.uk/fsl/fslwiki). The skeletonized MD maps were normalized to the FMRIB58 FA template in MNI space, using the spatial normalization routine and standard parameters of TBSS.[40] Then the obtained MD maps were multiplied with a conservatively defined binary white matter skeleton mask adopted from the TBSS toolbox to reduce partial volume effects, excluding the fornix and other regions susceptible to such effects, as described previously.[41] For the extraction of fiber tract ROI values of MD, the binarized Johns-Hopkins University fiber tract atlas[42] in MNI space was superimposed onto each subject's skeletonized MD map and the mean MD was computed for each fiber tract ROI.

2.9 | White matter hyperintensity measurement and probability mapping

White matter hyperintensities (as defined by the standards for reporting vascular changes on neuroimaging (STRIVE) criteria)[43] were segmented based on FLAIR MRI scans, using a semiautomated method that was described previously.[44] (For a more detailed description see

supplementary methods.) Global white matter hyperintensity (WMH) volume was computed by summing the voxels classified as WMH and multiplying the resulting sum by the voxel size of the native FLAIR scan. The total WMH volume was divided by the total brain volume to obtain a normalized global WMH volume (henceforth called WMH ratio). Because WMHs typically have a very skewed distribution, we applied an inverse-hyperbolic sine transform to the WMH volume ratio, as reported previously.[7]

WMH probability maps were separately computed for Aβ− and Aβ+ groups stratified by four age groups in order to display the age-related distribution of WMH: (1) 46 to 59 years, (2) 60 to 69 years, (3) 70 to 79 years, and (4) 80 to 89 years. Unlike in the previous analyses, where the age of the subjects was unrestricted between 30 and 89 years, for this particular analysis, a higher age limit was chosen as the age of the youngest Aβ+ subject (46 years), resulting in the sample size n = 254 (167 Aβ−, 87 Aβ+). Within each group, the spatially normalized and binarized WMH maps were concatenated across subjects. For each voxel, the number of subjects showing a WMH was counted, and this number was divided by the total number of subjects in the group to obtain the proportion of WMH occurrences for each voxel.

2.10 | Data analysis

2.10.1 | TBSS analysis of the effect of age and Aβ on MD

To test whether any observed association between age and MD was moderated by the presence of Aβ deposition, we conducted TBSS-based regression analyses including voxel values of MD as the dependent variable and the interaction age by Aβ status (Aβ− vs Aβ+) as the main predictor, controlled for age, Aβ status, sex, and education. Statistical significance was determined based on the Randomise Toolbox of FSL,[45] conducting nonparametric permutation inference using threshold-free cluster enhancement (TFCE; recommended for TBSS analyses) to correct for family-wise error (FWE).

In order to assess whether some patients had abnormal cognitive performance, we expressed each patient's composite score of episodic memory and executive function in terms of SD) from the group mean. Composite scores were adjusted by age, gender, and years of education as described in,[3] using linear regression. The linear regression equations were:

$$z_{adj}(i) = z_{raw}(i) - \left(B_{age} \times (age(i) - mean(age))\right) + B_{gender} \times (Gender(i) - Gender0) + B_{edu} \times (Education(i) - mean(Education))$$

z_{raw} (i) is the unadjusted composite score for subject (i) and similarly for z_{adj} (i), age (i), Gender (i) and Education (i). Gender0 represents the Gender reference value (female) and B_{age}, B_{gender}, and B_{edu} represent the linear regression coefficients for age, gender, and years of education, respectively.

We considered subjects with $z_{adj} < -1.5$ (ie, 1.5 SDs below the adjusted mean) in either episodic memory or executive function as potentially not cognitively healthy.

Results showed that in total, 4 of 282 (1 Aβ− and 1 Aβ+) were below the episodic memory threshold only.

2.11 | ROI-based analysis of the effect of age and Aβ on MD

We tested the same linear regression models as described earlier for the TBSS analysis on the interaction age by Aβ status on MD, this time having fiber tract ROI values of MD as the dependent variables. In additional linear regression analyses we tested whether any interaction effect of Aβ status x age remained when controlling for hypertension (note that for one patient the blood pressure measurement was missing). Because the tract-ROI–based analyses of MD was a secondary analysis, a significance threshold of $P < 0.05$ uncorrected for multiple comparisons was applied. Effect size f^2 was computed for the age and age x Aβ status terms.

2.12 | Assessing the influence of the APOE genotype

We tested whether the APOE ε4 genotype (ε4 carrier vs no ε4 carrier) was associated with the main predictors, that is, age (through a *t* test) and Aβ PET status (via chi-square).

In a TBSS analysis, APOE genotype and interaction term APOE genotype x age were tested as predictors of MD, controlled for age, gender, and education, using non-parametric permutation inference using threshold-free cluster enhancement (TFCE; recommended for TBSS analyses) to correct for family-wise error (FWE), with a corrected significance threshold of $\alpha = 0.05$.

2.13 | Analysis of the effect of age and Aβ on WMH

To assess the effect of Aβ status on WMH burden, we formulated a regression model with transformed WMH volume ratio as the dependent variable and the interaction age x Aβ status as the main predictor, with the rest of the covariates as per subsequent text. Because the inverse hyperbolic-sine transformation still resulted in a skewed distribution of WMH volume (with many patients showing few to no WMH), we used robust linear regression including weighted least squares, as implemented in the R package MASS.[46]

3 | RESULTS

3.1 | Patients' characteristics

Patients' characteristics are displayed in Table 1 for the Aβ groups. Aβ+ patients were older (t = 6.4, $P < 0.001$) and had lower executive

TABLE 1 Characteristics of patients with normal (Aβ−) and abnormal (Aβ+) amyloid PET

	Aβ− (n = 195)	Aβ+ (n = 87)	*P*-value
Sex (female)	117 (60%)	56 (64%)	$P = 0.595$
APOE ε4 status (carriers)	36 (20%)[b]	20 (25%)[b]	$P = 0.573$
Ethnicity[2]			
White/Caucasian	170	79	$P = 0.314$[3]
African American/Black	12	4	
Other	11	2	
Age in years (mean ± SD)/range	60.7 ± 13.5/30 – 88	70.3 ± 10.8/46 – 89	$P < 0.001$
Years of education (mean ± SD)	15.4 ± 2.2	15.6 ± 2.3	$P = 0.551$
Composite episodic memory score (mean ± SD)	0.08 ± 0.82	−0.16 ± 0.75	$P = 0.009$
Composite executive function score (mean ± SD)	0.10 ± 0.77	−0.24 ± 0.77	$P < 0.001$
Brain volume in mm^3 (median ± SD; $\times 10^6$)	1.37 ± 0.14	1.38 ± 0.12	$P = 0.052$
White matter volume in mm^3 (mean ± SD; $\times 10^5$)	4.97 ± 0.67	5.01 ± 0.63	$P = 0.001$
WMH volume in mm^3 (median ± IQR; $\times 10^{-3}$)	2.31 ± 3.5	5.19 ± 9.92	$P < 0.001$
WMH volume ratio (median ± IQR; $\times 10^{-3}$)	1.71 ± 2.76	4.06 ± 7.30	$P < 0.001$
Blood pressure, systolic, in mm Hg (mean ± SD)	127.9 ± 17.4	130.6 ± 17.3	$P = 0.176$
Blood pressure, diastolic, in mm Hg (mean ± SD)	81.3 ± 10.1	82.0 ± 9.0	$P = 0.583$
Number of patients with hypertension	74 (38%)[a]	36 (31%)	$P = 0.584$
Number of patients with treated hypertension	49 (66%)	27 (75%)	$P = 0.474$

Abbreviations: IQR, interquartile range (for non-normally distributed variables); SD, standard deviation (for approximately normally distributed variables).
[a]One subject lacked information on hypertension.
[b]Fifteen Aβ− patients and 7 Aβ+ subjects did not have APOE genotyping available. Percentages are show over the total number of patients with available APOE genotyping per Aβ group. Tests: χ^2-test for categorical variables, *t* tests for age and education, analysis of covariance (ANCOVA) for all other continuous variables, controlled for age, sex, years of education and, in case of gray matter (GM) and white matter (WM) volume, total intracranial volume.

function composite scores (t = −3.4, $P < 0.001$) than Aβ− patients. APOE genotype was neither associated with age ($P = 0.31$) nor with Aβ PET status ($P = 0.57$).

3.2 | TBSS analysis of the effect of age and Aβ status on MD

TBSS analysis showed a significant Aβ status x age interaction for MD. In Aβ+ patients, higher age was associated with a stronger increase in MD compared to that in Aβ− patients. The peak interaction effects of Aβ status x age were located predominantly within the posterior parietal white matter including fiber tracts such as the forceps major and long-projecting fibers connecting posterior brain regions (Figure 1, Table 2). The results remained virtually unchanged when excluding those four patients who scored <1.5 SD below the mean on the composite scores of episodic memory or executive function, suggesting that the findings were not driven by abnormally low-performing subjects. When using global Aβ PET SUVR as a continuous rather than binary measure, the interaction effect global Aβ PET SUVR x age on MD remained significant in the same tracts (except for the anterior thalamic radiation, Supplementary Figure S1 and Supplementary Table S1), albeit in a more spatially restricted manner.

TBSS analysis of the effect of APOE genotype x age interaction on MD values did not yield any significant results (data not shown).

3.3 | ROI-based analysis of the effect of age and Aβ on MD

When analyzed at the fiber-tract ROI level, Aβ+ status was associated numerically with higher age-related increase in MD within multiple tracts that were largely consistent with the location of significant voxel clusters of the interaction effect reported in the TBSS analysis (Supplementary Figure S2, Supplementary Table S2). However, the test of the interaction effects were not statistically significant after Bonferroni correction. This was probably because MD alterations were observed only in parts of a tract, so that averaging the MD values across all voxels of a tract diluted the effect and thus reduced statistical power.

Linear regression analysis of the interaction effect of APOE genotype x age did not yield significant results for any of the fiber tracts (data not shown).

3.4 | Analysis of the effect of age and Aβ on WMH

Probability mapping of WMH for Aβ− and Aβ+ groups for different age decades starting at age 46 years is displayed in Figure 2 (for WMH in patients 30-46 years of age, see Supplementary Figure S3). In both groups, WMH occurred predominantly in the periventricular white matter. Regression analysis showed a significant interaction Aβ status x age on the global WMH ratio (B = 0.30, standard error [SE] = 0.14, 95%

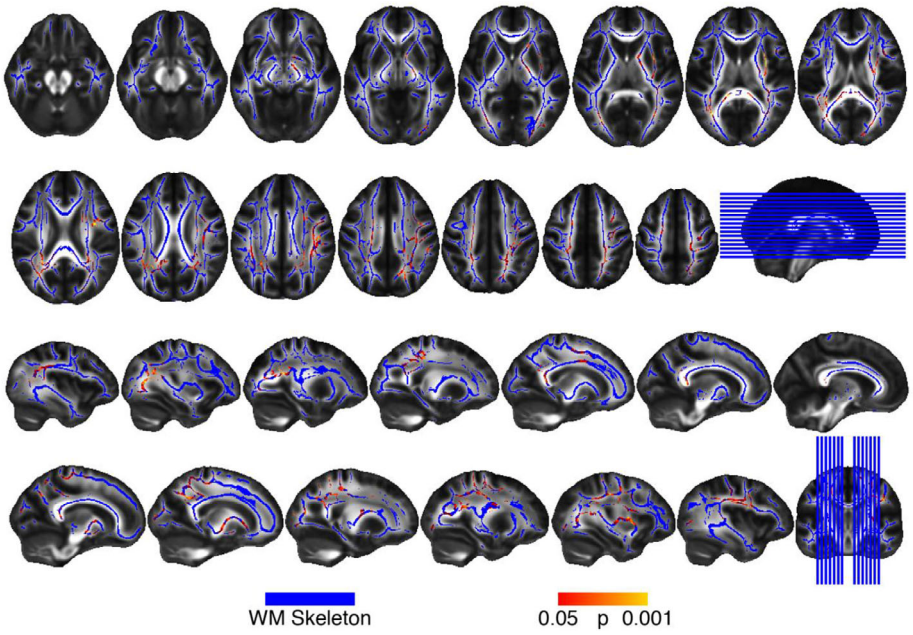

FIGURE 1 TBSS map of the interaction effect of age x global Aβ PET status (Aβ− vs Aβ+) on MD within the white matter (WM) skeleton (blue) in the axial view (upper two rows) and sagittal view (lower two rows). At higher levels of global amyloid PET, age was associated with a stronger increase in MD than at lower levels of global amyloid PET. No interaction effects were observed in the opposite direction. *P*-values associated with the interaction effect are encoded in warm colors (red to yellow); the significance level was $P < 0.05$ FWE corrected

TABLE 2 Voxel-based analysis: anatomical labels, coordinates in MNI space, and *t* value of the TBSS-derived peaks of each cluster of the interaction effects of Aβ PET status by age on MD

Tract	Lobe/side	X	Y	Z	*t* value
Inferior frontooccipital fasciculus	Parietal/L	−29	−45	18	4.81
Superior longitudinal fasciculus	Frontal/R	36	−15	34	4.41
Superior longitudinal fasciculus	Parietal/R	21	−44	47	3.77
Superior longitudinal fasciculus	Temporal/R	32	−2	13	3.96
Cingulum	Parietal/R	19	−54	36	4.04
Forceps major	Parietal	17	−43	10	4.30
Inferior longitudinal fasciculus	Parietal/R	27	−42	25	4.04

Abbreviations: L, left, R, right.

confidence interval [CI] = 0.07-0.59, $P = 0.026$), such that the association between higher age and higher global WMH ratio was stronger in the Aβ+ compared to the Aβ− group (Figure 3). To ensure that zero or very low values of WMH volume did not influence the results, we repeated the regression analysis with cases of WMH volume below the fifth percentile (n = 25) excluded (B = 0.29, SE = 0.14, 95% CI = 0.02-0.58, $P = 0.037$). The interaction effect remained also significant when controlling for hypertension (full sample: B = 0.33, SE = 0.13, 95% CI = 0.07-0.59, $P = 0.015$), where hypertension had no significant effect on WMH ratio (data not shown).

4 | DISCUSSION

The major results of the current adult life span study in cognitively normal subjects (30-89 years) showed abnormal global Aβ deposition (global Florbetapir F-18 PET) to be associated with stronger age-related MD alterations, particularly within the posterior parietal white matter. Aβ+ status was also associated with stronger age-related increase in global WMH volume, independent of hypertension. Together, these results suggest that Aβ deposition is associated with white matter alterations throughout the adult life span in cognitively normal subjects.

Increased MD in the posterior parietal white matter included fiber tracts such as the forceps major, inferior frontooccipital fasciculus, and superior longitudinal fasciculus. These fiber tracts connect among others regions of the default mode network (DMN),[47] that is, a major functional network impaired in both cognitively normal subjects with elevated Aβ levels[48,49] and patients with AD dementia.[50] White matter alterations in tracts connecting the DMN were shown previously to be associated with reduced functional connectivity in patients with AD,[44] suggesting that white matter

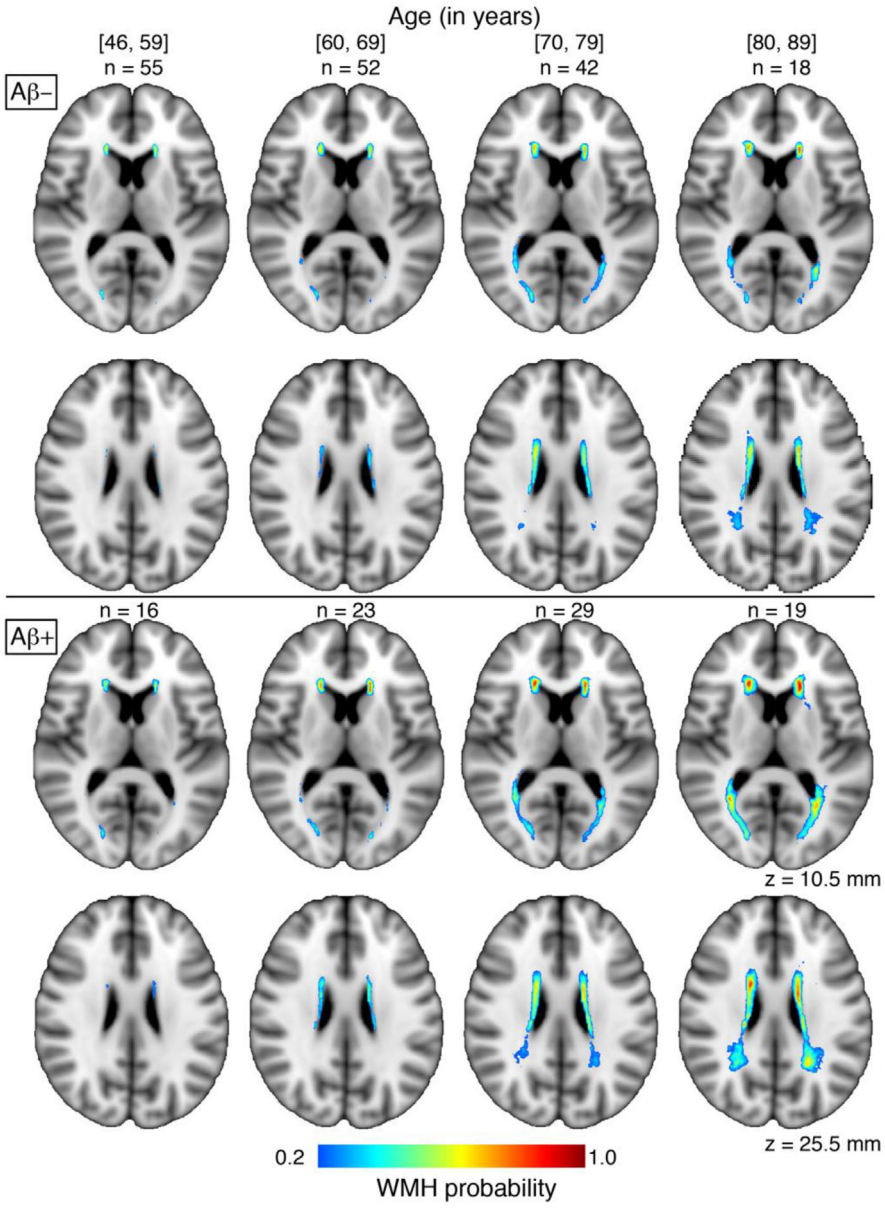

FIGURE 2 WMH probability maps superimposed onto axial brain slices within the Aβ− group (upper panel) and Aβ+ group (lower panel) for different age groups (columns). The number of subjects per Aβ and age group is indicated above the slices

alterations contribute to impairment in key functional networks in AD.

The posterior parietal spatial distribution of MD alterations observed in the current study shows a spatial similarity to that previously found in mild AD[51,52] (for review see[53]), and in subjects with autosomal dominant AD.[13] In autosomal dominant AD, we previously reported higher MD within the forceps major 10 years before symptom onset, with other major long-projecting fibers tracts such as the inferior frontooccipital fasciculus, superior longitudinal fasciculus, and forceps minor affected subsequently.[13] Similarly, in the current study, we observed significant amyloid-related MD increase that was located primarily in temporal and posterior brain regions. It should be noted that the white matter alterations extended to frontal fiber tracts such as the anterior thalamic radiation. Alterations in the frontal white matter, including among other regions the anterior thalamic radiation, have been reported previously in late-onset AD.[54,55] It is thus possible that due to the age difference between autosomal dominant Alzheimer's disesae compared to late onset AD,[13] more frontal white matter alterations are present in late-onset AD. Whether regional differences in Aβ PET contribute to regionally matching differences in MD alterations was not possible to address in the current study, given that local Aβ PET values are highly intercorrelated and thus regional Aβ PET changes are difficult to disentangle from global Aβ PET changes.

The underlying mechanisms of Aβ-related MD alterations remain unclear. One possibility is that the deposition of Aβ enhances small vessel disease, in the form of cerebral amyloid angiopathy (CAA). White matter damage in AD might thus be related to vascular mechanisms, such as hypoperfusion (for reviews see[6,56]). Cerebrovascular

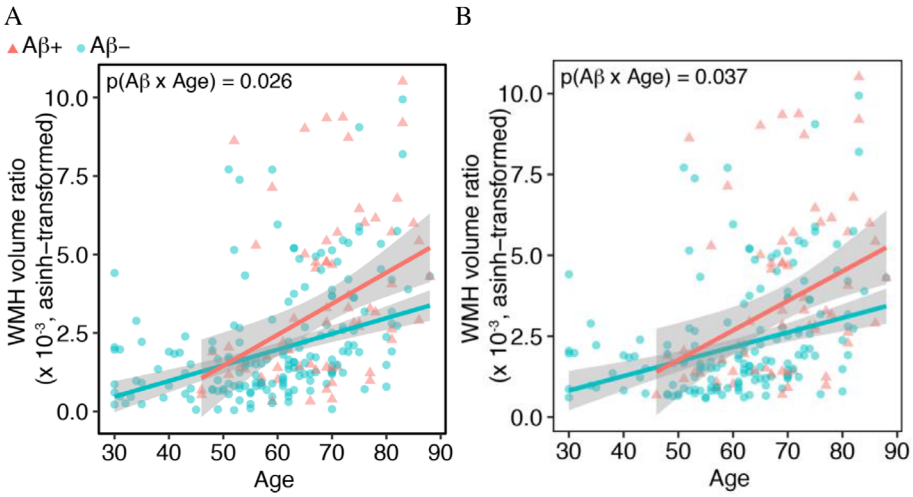

FIGURE 3 Regression plot showing the interaction between Aβ status x age on global WMH volume ratio for the full sample (A) and the subset of subjects, excluding those falling below the fifth percentile of WMH volume (B) to ensure that the results were not driven by zero (or very low) WMH volume. The shaded area indicates the standard error

pathology such as CAA occurs in the majority of patients with AD,[57] and its prevalence is also increased in cognitively normal subjects exhibiting neuritic amyloid plaques.[58] Aβ induces vasoconstriction and reduces functional hyperemia, as observed in mouse models of cerebral Aβ deposition.[56,59] Furthermore, higher parenchymal Aβ may enhance CAA and associated perfusion alterations.[60] Microstructural white matter alterations becoming visible as WMH have been associated previously with small vessel disease changes including capillary CAA and hypoperfusion.[21,61] In the current study, we found higher age-related increase in WMH volume in subjects with abnormal Florbetapir F-18 PET levels compared to those with normal Florbetapir F-18 PET. Consistent with our results, relatively young patients with autosomal dominant AD showed an increase in WMH subsequent to amyloid deposition,[7] suggesting that amyloid pathology may entail white matter alterations. In humans, arterial spin labeling studies showed that lower tissue perfusion was associated not only with WMH volume but also DTI alterations in fiber tracts outside the WMH.[62] Together, these results suggest that Aβ-related small vessel disease constitutes a potential pathomechanism underlying the microstructural fiber tract alterations observed in the current study.

Hypertension is an age-related cerebrovascular risk factor and may thus enhance the risk of white matter alterations. In addition, cerebrovascular disease has been suggested to enhance the development of AD,[63] and thus hypertension may not only be a vascular risk factor but also a risk factor for enhanced accumulation of Aβ in the brain.[18] In our study, the effects of Aβ on both MD alterations and WMH were, however, independent of the hypertension status, suggesting that hypertensive small vessel disease does not account for the observed effects on white matter. It is still possible that hypertension enhances the development of Aβ[18] and exacerbates Aβ-related small vessel disease,[64] but in the current study, hypertension was not the major determinant. We caution, however, that in the majority of cases hypertension was treated, and thus any effects of hypertension may have been attenuated by treatment. Multiple sources may synergistically contribute to white matter alterations and cognitive decline,[65-67] where future studies need to address the causative relationship and mechanistic pathways between these factors.

For the interpretation of the current study, some caveats should be considered. Although an increase in MD is commonly thought to reflect decreased fiber tract integrity, the exact sources of changes in DTI signal are not well understood.[68,69] Changes in MD may be influenced by changes in crossing fibers[10,68,69] or an increase in extracellular free water without pronounced alterations of fiber tract structure itself,[70] which complicates the attribution of MD differences to underlying changes in fiber tract integrity. Multishell acquisition protocols and free water elimination have been developed[71-73] to alleviate such shortcomings; however, this work is ongoing.[74] Furthermore, we focused on MD only, and our results do not necessarily generalize to other DTI indices such as fractional anisotropy (FA), even though we found that MD and FA were highly correlated in our data set (data not shown). Another caveat is that the current study does not include longitudinal data, which would be instructive to establish the temporal sequence of age-related development of Aβ and white matter changes during the adult life span.[63,75] Reduced perfusion and impaired blood-brain barrier function have been proposed to precede the development of Aβ.[1,56,57] Furthermore, small vessel disease may interact with Aβ pathology, and thus exacerbate the development of AD pathology.[64,76] The current cross-sectional findings cannot disentangle the directionality of the effect that white matter alterations, possibly stemming from small vessel disease, and Aβ pathology may exert on each other.

Lastly, we note that while our results suggest Aβ to be associated with white matter alterations at higher age, one alternative possibility is that the association between Aβ and white matter alterations becomes better detectable at higher age, where white matter integrity is more variable. Biological factors that may enhance the association between Aβ and white matter alterations specifically at higher age remain still unclear.

In conclusion, the current study shows that the occurrence of Aβ deposition is associated with an age-related increase in white matter alterations. Our results have clinical implications. Small vessel disease is treatable, and interventions enhancing vascular health at an early disease stage may thus alleviate disease progression in patients with increased levels of Aβ.[77] Recently developed, clinically applicable neuroimaging markers of white matter damage[41] could help track white matter alterations and treatment effects, both in response to vascular or Aβ-targeted intervention for secondary prevention.

FUNDING/SUPPORT

The study was supported by the Alzheimer's Association (to M.E.), European Research Council PCIG12-GA-2012-334259 (to M.E), LMUexcellent (to M.E.), National Institute on Aging 5R37AG-006265 (to D.P.) and RC1AG036199 (to D.P.). The PETtracer was provided at no cost by Avid Radiopharmaceuticals, a wholly owned subsidiary of Eli Lilly, Inc, which had no role in the design and conduct of the study, analysis of the data, or manuscript preparation.

CONFLICT OF INTEREST

No conflicts of interest were reported by any author.

ORCID

Michael Ewers https://orcid.org/0000-0001-5231-1714

REFERENCES

1. Zlokovic BV. Neurovascular pathways to neurodegeneration in Alzheimer's disease and other disorders. *Nat Rev Neurosci*. 2011; 12:723-738.
2. Thal DR, Attems J, Ewers M. Spreading of amyloid, tau, and microvascular pathology in Alzheimer's disease: findings from neuropathological and neuroimaging studies. *J Alzheimers Dis*. 2014;42(suppl 4): S421-S429.
3. Jacobs HIL, Hedden T, Schultz AP, et al. Structural tract alterations predict downstream tau accumulation in amyloid-positive older individuals. *Nat Neurosci*. 2018;21(3):424-431.
4. Mito R, Raffelt D, Dhollander T, et al. Fibre-specific white matter reductions in Alzheimer's disease and mild cognitive impairment. *Brain*. 2018;141(3):888-902.
5. Song SK, Kim JH, Lin SJ, Brendza RP, Holtzman DM. Diffusion tensor imaging detects age-dependent white matter changes in a transgenic mouse model with amyloid deposition. *Neurobiol Dis*. 2004;15:640-647.
6. Weller RO, Boche D, Nicoll JA. Microvasculature changes and cerebral amyloid angiopathy in Alzheimer's disease and their potential impact on therapy. *Acta Neuropathol*. 2009;118:87-102.
7. Lee S, Viqar F, Zimmerman ME, et al. White matter hyperintensities are a core feature of Alzheimer's disease: evidence from the dominantly inherited Alzheimer network. *Ann Neurol*. 2016;79:929-939.
8. Medina D, DeToledo-Morrell L, Urresta F, et al. White matter changes in mild cognitive impairment and AD: a diffusion tensor imaging study. *Neurobiol Aging*. 2006;27:663-672.
9. Sexton CE, Kalu UG, Filippini N, Mackay CE, Ebmeier KP. A meta-analysis of diffusion tensor imaging in mild cognitive impairment and Alzheimer's disease. *Neurobiol Aging*. 2011;32:2322.e5-18.
10. Douaud G, Jbabdi S, Behrens TE, et al. DTI measures in crossing-fibre areas: increased diffusion anisotropy reveals early white matter alteration in MCI and mild Alzheimer's disease. *Neuroimage*. 2011;55:880-890.
11. Caso F, Agosta F, Filippi M. Insights into white matter damage in Alzheimer's disease: from postmortem to in vivo diffusion tensor MRI studies. *Neurodegener Dis*. 2016;16:26-33.
12. Bendlin BB, Carlsson CM, Johnson SC, et al. CSF T-Tau/Abeta42 predicts white matter microstructure in healthy adults at risk for Alzheimer's disease. *PLoS One*. 2012;7:e37720.
13. Araque Caballero MA, Suarez-Calvet M, Duering M, et al. White matter diffusion alterations precede symptom onset in autosomal dominant Alzheimer's disease. *Brain*. 2018;141:3065-3080.
14. Sachdev PS, Zhuang L, Braidy N, Wen W. Is Alzheimer's a disease of the white matter?. *Curr Opin Psychiatry*. 2013;26:244-251.
15. Oxtoby NP, Young AL, Cash DM, et al. Data-driven models of dominantly-inherited Alzheimer's disease progression. *Brain*. 2018;141:1529-1544.
16. Bateman RJ, Xiong C, Benzinger TL, et al. Clinical and biomarker changes in dominantly inherited Alzheimer's disease. *N Engl J Med*. 2012;367:795-804.
17. Jansen WJ, Ossenkoppele R, Knol DL, et al. Prevalence of cerebral amyloid pathology in persons without dementia: a meta-analysis. *JAMA*. 2015;313:1924-1938.
18. Rodrigue KM, Rieck JR, Kennedy KM, Devous MD, Sr, Diaz-Arrastia R, Park DC. Risk factors for beta-amyloid deposition in healthy aging: vascular and genetic effects. *JAMA Neurol*. 2013;70:600-606.
19. Mann DMA, Davidson YS, Robinson AC, et al. Patterns and severity of vascular amyloid in Alzheimer's disease associated with duplications and missense mutations in APP gene, Down syndrome and sporadic Alzheimer's disease. *Acta Neuropathol*. 2018;136(4): 569-587.
20. Paradise MB, Shepherd CE, Wen W, Sachdev PS. Neuroimaging and neuropathology indices of cerebrovascular disease burden: a systematic review. *Neurology*. 2018;91:310-320.
21. Charidimou A, Martinez-Ramirez S, Reijmer YD, et al. Total magnetic resonance imaging burden of small vessel disease in cerebral amyloid angiopathy: an imaging-pathologic study of concept validation. *JAMA Neurol*. 2016;73:994-1001.
22. van Veluw SJ, Lauer A, Charidimou A, et al. Evolution of DWI lesions in cerebral amyloid angiopathy: evidence for ischemia. *Neurology*. 2017;89:2136-2142.
23. Lebel C, Gee M, Camicioli R, Wieler M, Martin W, Beaulieu C. Diffusion tensor imaging of white matter tract evolution over the lifespan. *Neuroimage*. 2012;60:340-352.
24. Kochunov P, Williamson DE, Lancaster J, et al. Fractional anisotropy of water diffusion in cerebral white matter across the lifespan. *Neurobiol Aging*. 2012;33:9-20.
25. Hasan KM, Iftikhar A, Kamali A, et al. Development and aging of the healthy human brain uncinate fasciculus across the lifespan using diffusion tensor tractography. *Brain Res*. 2009;1276:67-76.
26. Dean DC, 3rd, Hurley SA, Kecskemeti SR, et al. Association of amyloid pathology with myelin alteration in preclinical Alzheimer disease. *JAMA Neurol*. 2017;74:41-49.
27. Song Z, Farrell ME, Chen X, Park DC. Longitudinal accrual of neocortical amyloid burden is associated with microstructural changes of the fornix in cognitively normal adults. *Neurobiol Aging*. 2018;68: 114-122.
28. Racine AM, Merluzzi AP, Adluru N, et al. Association of longitudinal white matter degeneration and cerebrospinal fluid biomarkers of neurodegeneration, inflammation and Alzheimer's disease in late-middle-aged adults. *Brain Imaging Behav*. 2019;13(1):41-52.
29. Gold BT, Zhu Z, Brown CA, et al. White matter integrity is associated with cerebrospinal fluid markers of Alzheimer's disease in normal adults. *Neurobiol Aging*. 2014;35:2263-2271.
30. Chao LL, Decarli C, Kriger S, et al. Associations between white matter hyperintensities and beta amyloid on integrity of projection, association, and limbic fiber tracts measured with diffusion tensor MRI. *PLoS One*. 2013;8:e65175.

31. Rieckmann A, Van Dijk KR, Sperling RA, Johnson KA, Buckner RL, Hedden T. Accelerated decline in white matter integrity in clinically normal individuals at risk for Alzheimer's disease. *Neurobiol Aging*. 2016;42:177-188.
32. Racine AM, Adluru N, Alexander AL, et al. Associations between white matter microstructure and amyloid burden in preclinical Alzheimer's disease: a multimodal imaging investigation. *NeuroImage Clinical*. 2014;4:604-614.
33. Li X, Li TQ, Andreasen N, Wiberg MK, Westman E, Wahlund LO. The association between biomarkers in cerebrospinal fluid and structural changes in the brain in patients with Alzheimer's disease. *J Intern Med*. 2014;275:418-427.
34. Song Z, McDonough IM, Liu P, Lu H, Park DC. Cortical amyloid burden and age moderate hippocampal activity in cognitively-normal adults. *NeuroImage Clinical*. 2016;12:78-84.
35. Rodrigue KM, Kennedy KM, Devous MD, et al. β-Amyloid burden in healthy aging. *Neurology*. 2012;78:387-395.
36. Bischof GN, Jessen F, Fliessbach K, et al. Impact of tau and amyloid burden on glucose metabolism in Alzheimer's disease. *Ann Clin Transl Neurol*. 2016;3:934-939.
37. Leemans A, Jeurissen B, Sijbers J, Jones D, *ExploreDTI: a graphical toolbox for processing, analyzing, and visualizing diffusion MRI data*. Proceedings of the 17th Annual Meeting of International Society for Magnetic Resonance in Medicine Hawaii, USA. 2009, pp. 3536.
38. Leemans A, Jones DK. The B-matrix must be rotated when correcting for subject motion in DTI data. *Magn Reson Med*. 2009;61:1336-1349.
39. Irfanoglu MO, Walker L, Sarlls J, Marenco S, Pierpaoli C. Effects of image distortions originating from susceptibility variations and concomitant fields on diffusion MRI tractography results. *Neuroimage*. 2012;61:275-288.
40. Smith SM, Jenkinson M, Johansen-Berg H, et al. Tract-based spatial statistics: voxelwise analysis of multi-subject diffusion data. *Neuroimage*. 2006;31:1487-1505.
41. Baykara E, Gesierich B, Adam R, et al. A novel imaging marker for small vessel disease based on skeletonization of white matter tracts and diffusion histograms. *Ann Neurol*. 2016;80:581-592.
42. Hua K, Zhang J, Wakana S, et al. Tract probability maps in stereotaxic spaces: analyses of white matter anatomy and tract-specific quantification. *Neuroimage*. 2008;39:336-347.
43. Wardlaw JM, Smith EE, Biessels GJ, et al. Neuroimaging standards for research into small vessel disease and its contribution to ageing and neurodegeneration. *Lancet Neurol*. 2013;12:822-838.
44. Taylor AN, Kambeitz-Ilankovic L, Gesierich B, et al. Tract-specific white matter hyperintensities disrupt neural network function in Alzheimer's disease. *Alzheimers Dement*. 2017;13:225-235.
45. Winkler AM, Ridgway GR, Webster MA, Smith SM, Nichols TE. Permutation inference for the general linear model. *Neuroimage*. 2014;92:381-397.
46. Venables WN, Ripley BD. Modern Applied Statistics With S. 4th ed. New York City: Springer; 2002.
47. Greicius MD, Supekar K, Menon V, Dougherty RF. Resting-state functional connectivity reflects structural connectivity in the default mode network. *Cereb Cortex*. 2009;19:72-78.
48. Wang L, Brier MR, Snyder AZ, et al. Cerebrospinal fluid Abeta42, phosphorylated Tau181, and resting-state functional connectivity. *JAMA Neurol*. 2013;70:1242-1248.
49. Elman JA, Madison CM, Baker SL, et al. Effects of beta-amyloid on resting state functional connectivity within and between networks reflect known patterns of regional vulnerability. *Cereb Cortex*. 2016;26:695-707.
50. Badhwar A, Tam A, Dansereau C, Orban P, Hoffstaedter F, Bellec P. Resting-state network dysfunction in Alzheimer's disease: a systematic review and meta-analysis. *Alzheimers Dement*. 2017;8:73-85.
51. Acosta-Cabronero J, Alley S, Williams GB, Pengas G, Nestor PJ. Diffusion tensor metrics as biomarkers in Alzheimer's disease. *PLoS One*. 2012;7:e49072.
52. Acosta-Cabronero J, Williams GB, Pengas G, Nestor PJ. Absolute diffusivities define the landscape of white matter degeneration in Alzheimer's disease. *Brain*. 2010;133:529-539.
53. Acosta-Cabronero J, Nestor PJ. Diffusion tensor imaging in Alzheimer's disease: insights into the limbic-diencephalic network and methodological considerations. *Front Aging Neurosci*. 2014;6:266.
54. Niida A, Niida R, Kuniyoshi K, Motomura M, Uechi A. Usefulness of visual evaluation of the anterior thalamic radiation by diffusion tensor tractography for differentiating between Alzheimer's disease and elderly major depressive disorder patients. *Int J Gen Med*. 2013;6:189-200.
55. Tu MC, Lo CP, Huang CF, et al. Effectiveness of diffusion tensor imaging in differentiating early-stage subcortical ischemic vascular disease, Alzheimer's disease and normal ageing. *PLoS One*. 2017;12:e0175143.
56. Kisler K, Nelson AR, Montagne A, Zlokovic BV. Cerebral blood flow regulation and neurovascular dysfunction in Alzheimer disease. *Nat Rev Neurosci*. 2017;18:419-434.
57. Iadecola C. The pathobiology of vascular dementia. *Neuron*. 2013;80:844-866.
58. Jicha GA, Abner EL, Schmitt FA, et al. Preclinical AD Workgroup staging: pathological correlates and potential challenges. *Neurobiol Aging*. 2012;33:622.e1-e16.
59. Niwa K, Younkin L, Ebeling C, et al. Abeta 1-40-related reduction in functional hyperemia in mouse neocortex during somatosensory activation. *PNAS*. 2000;97:9735-9740.
60. Maier FC, Wehrl HF, Schmid AM, et al. Longitudinal PET-MRI reveals beta-amyloid deposition and rCBF dynamics and connects vascular amyloidosis to quantitative loss of perfusion. *Nat Med*. 2014;20:1485-1492.
61. Shi Y, Thrippleton MJ, Makin SD, et al. Cerebral blood flow in small vessel disease: a systematic review and meta-analysis. *J Cereb Blood Flow Metab*. 2016;36:1653-1667.
62. Promjunyakul N, Lahna D, Kaye JA, et al. Characterizing the white matter hyperintensity penumbra with cerebral blood flow measures. *NeuroImage Clinical*. 2015;8:224-229.
63. Iturria-Medina Y, Sotero RC, Toussaint PJ, Mateos-Perez JM, Evans AC, Alzheimer's Disease Neuroimaging Initiative. Early role of vascular dysregulation on late-onset Alzheimer's disease based on multifactorial data-driven analysis. *Nat Commun*. 2016;7:11934.
64. Faraco G, Park L, Zhou P, et al. Hypertension enhances Abeta-induced neurovascular dysfunction, promotes beta-secretase activity, and leads to amyloidogenic processing of APP. *J Cereb Blood Flow Metab*. 2016;36:241-252.
65. Rabin JS, Schultz AP, Hedden T, et al. Interactive associations of vascular risk and beta-amyloid burden with cognitive decline in clinically normal elderly individuals: findings from the Harvard Aging Brain Study. *JAMA Neurol*. 2018;75:1124-1131.
66. Lee MJ, Seo SW, Na DL, et al. Synergistic effects of ischemia and beta-amyloid burden on cognitive decline in patients with subcortical vascular mild cognitive impairment. *JAMA psychiatry*. 2014;71:412-422.
67. Vemuri P, Lesnick TG, Przybelski SA, et al. Vascular and amyloid pathologies are independent predictors of cognitive decline in normal elderly. *Brain*. 2015;138:761-771.
68. Jeurissen B, Leemans A, Tournier JD, Jones DK, Sijbers J. Investigating the prevalence of complex fiber configurations in white matter tissue with diffusion magnetic resonance imaging. *Hum Brain Mapp*. 2013;34:2747-2766.
69. Jones DK, Knosche TR, Turner R. White matter integrity, fiber count, and other fallacies: the do's and don'ts of diffusion MRI. *Neuroimage*. 2013;73:239-254.

70. Pasternak O, Sochen N, Gur Y, Intrator N, Assaf Y. Free water elimination and mapping from diffusion MRI. *Magn Reson Med*. 2009;62:717-730.
71. Zhang H, Schneider T, Wheeler-Kingshott CA, Alexander DC. NODDI: practical in vivo neurite orientation dispersion and density imaging of the human brain. *Neuroimage*. 2012;61:1000-1016.
72. Duering M, Finsterwalder S, Baykara E, et al. Free water determines diffusion alterations and clinical status in cerebral small vessel disease. *Alzheimers Dement*. 2018.
73. Maier-Hein KH, Westin CF, Shenton ME, et al. Widespread white matter degeneration preceding the onset of dementia. *Alzheimers Dement*. 2015;11:485-493.e2.
74. Hoy AR, Koay CG, Kecskemeti SR, Alexander AL. Optimization of a free water elimination two-compartment model for diffusion tensor imaging. *Neuroimage*. 2014;103:323-333.
75. Lo RY, Jagust WJ, Alzheimer's Disease Neuroimaging Initiative. Vascular burden and Alzheimer disease pathologic progression. *Neurology*. 2012;79:1349-1355.
76. Iadecola C, Zhang F, Niwa K, et al. SOD1 rescues cerebral endothelial dysfunction in mice overexpressing amyloid precursor protein. *Nat Neurosci*. 1999;2:157-161.
77. Iturria-Medina Y, Carbonell FM, Sotero RC, Chouinard-Decorte F, Evans AC, Alzheimer's Disease Neuroimaging Initiative. Multifactorial causal model of brain (dis)organization and therapeutic intervention: application to Alzheimer's disease. *Neuroimage*. 2017;152:60-77.
78. Otsu N. A threshold selection method from gray-level histograms. *IEEE Trans Syst Man Cybern*. 1979;9:62-66.
79. Ashburner J. A fast diffeomorphic image registration algorithm. *Neuroimage*. 2007;38:95-113.

SUPPORTING INFORMATION

Additional supporting information may be found online in the Supporting Information section at the end of the article.

How to cite this article: Caballero MÁA, Song Z, Rubinski A, et al. Age-dependent amyloid deposition is associated with white matter alterations in cognitively normal adults during the adult life span. *Alzheimer's Dement*. 2020;16:651–661. https://doi.org/10.1002/alz.12062